Background removal procedure based on the SNIP algorithm for γ -ray spectroscopy with the CAEN Educational Kit.

Massimo Caccia, Amedeo Ebolese, Matteo Maspero, Romualdo Santoro Dipartimento di Scienza e Alta Tecnologia,
Universita' degli Studi dell'Insubria, 22100, Como, Italy
Marco Locatelli, Maura Pieracci, Carlo Tintori
CAEN S.p.A., 55049, Viareggio, Italy

Abstract—In gamma spectra the energy, the intensity and the number of resolved photo peaks depend on the detector resolution and the background from physics processes. A widely used method for subtracting the background under a photopeak is provided by the Sensitive Nonlinear Iterative Peak (SNIP) algorithm. This paper reports a validation procedure of the SNIP algorithm, based on the invariance of the photo-peak area for different background levels.

Index Terms—Silicon Photo Multipliers, gamma ray spectroscopy

I. INTRODUCTION

AMMA-RAY spectroscopy is relevant in basic and applied fields of science and technology, from nuclear to medical physics, from archaeometry [1], [2] to homeland security [3], [4].

In recorded γ —spectra of radioactive samples the number of resolved photo-peaks and the measurement of their energy and intensity is affected by the detector resolution and by background physics processes. In general, the characterization of the photo-peaks implies a robust estimation of the underlying background. Several approaches have been proposed, going from a simple estimate by an analysis of the side bands of the peaks to a spectrum fit with an analytical description of the background.

A flexible and widely used method is provided by the Sensitive Nonlinear Iterative Peak (SNIP) algorithm [5]–[7]. This paper presents a validation procedure of the SNIP algorithm based on the invariance of the photo-peak area when the underlying background changes.

II. Background subtraction in $\gamma-\text{spectra}$

For energies of γ below the pair production, the interaction with the detector is dominated by Compton scattering and photo-absorption. Exemplary theoretical and experimental spectra are shown in Fig. 1. The Compton continuum is due to the recoiling electrons with energy

$$E_e = E_0 \times \left(\frac{\frac{E_0}{mc^2} (1 - cos\theta)}{1 + \frac{E_0}{mc^2} (1 - cos\theta)} \right),$$

Corresponding Authors: massimo.caccia@uninsubria.it, m locatelli@caen.it

where E_0 is the incoming γ -ray energy, θ is the scattering angle and mc^2 is the electron rest-mass. The experimental spectrum results by a smearing of the underlying physics distribution [8] [9], implying a photo-absorption peak broadening possibly contaminated by the edge of the Compton spectrum and referred as background in the following.

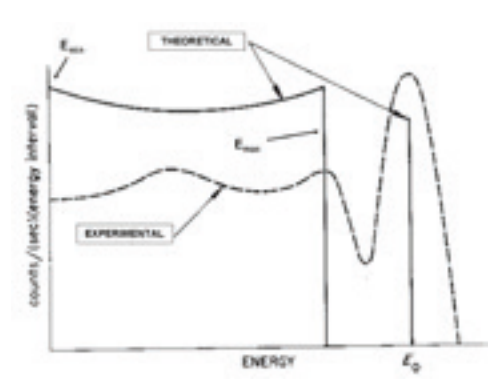


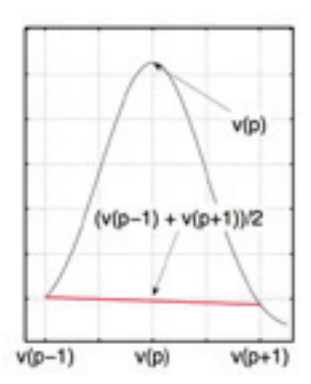
Fig. 1: Theoretical energy distribution for Compton and photoelectric interaction (continuous line) and experimental pulse-height distribution in a scintillation detector [8].

The photo-peaks are the signature of a spectrum. Their analysis conveys relevant information about the radioactive sample and the experimental apparatus:

- the peak energies are distinctive of the decaying nuclei in the sample;
- the area of peaks measure the relative concentrations of isotopes;
- the linearity of the system is provided by the spectra for a set of known γ emitters;
- the width of the peaks represents the electronics plus detector resolution. Its dependence against the energy accounts for the poissonian fluctuations in the signal and the detector response.

The SNIP algorithm has been introduced with the aim to separate useless information (i.e.: background, noise and detector artifacts) from useful information contained in the

peak.



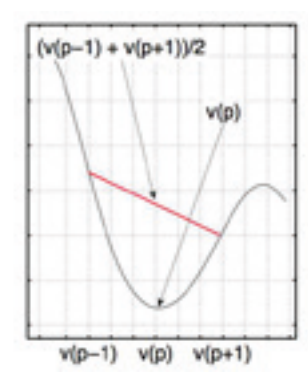


Fig. 2: Illustration of the SNIP algorithm applied to the peak region (left plot) and to a valley of the spectrum (right plot). Figure adapted from [7].

The core procedure of the SNIP [7] requires a preprocessing step, where the count y(i) in channel i-th is transformed according to:

$$y(i) \mapsto v(i) = log(log(\sqrt{y(i) + 1} + 1) + 1).$$

The square-root operator enhances small peaks while the double log operator was introduced to cope with complex spectra with relative intensities over several orders of magnitude.

The background under the peak is evaluated in an iterative way. For the M-th iteration, the content of the transformed bin $v_M(i)$ is compared to the mean of the values at distance equals to $\pm M$ and the updated spectrum is evaluated as:

$$v_{M+1}(i) = \min \left\{ v_M(i), \frac{v_M(i-M) + v_M(i+M)}{2} \right\}.$$

In proximity of peaks, as long as the distance is comparable to the peak width, the updated spectrum will result by the shape of the side bands. On the other hand, valleys will be essentially unchanged (see Fig. 2). An exemplary illustration of the outcome of the procedure is shown in Fig. 3, where the raw spectrum, the background estimated with SNIP and the spectrum with the subtracted background are overimposed. Fig. 3 clearly shows that the peak side wings fluctuate around zero as expected after a correct background subtraction.

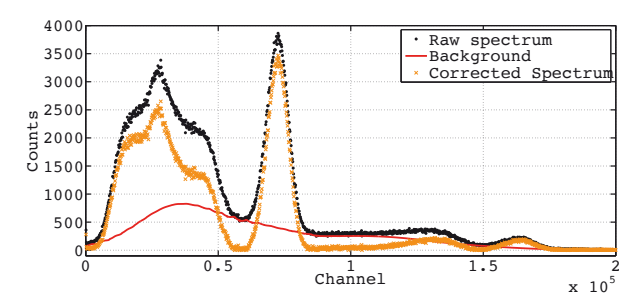


Fig. 3: Typical ²²Na gamma spectrum. The raw data are shown in black, the estimated background in red and the spectrum with the subtracted background in brown.

The main advantage of the SNIP algorithm is the capability to cope with a large variety of background shapes. Its potential weakness is in the absence of a built-in convergence criterion. In this specific application, the iterative procedure is stopped as long as the estimated background is monotonically changing in the peak region. As a complementary condition, essentially applied for low background spectra where the statistical fluctuations are dominating, the procedure is stopped as long as the background drops below 5% of the total area underneath the peak.

III. EXPERIMENTAL SET-UP

The experimental set-up is based on the CAEN Silicon PhotoMultiplier Educational Kit [10], a modular system for undergraduate experiments in nuclear science, photonics and statistics.



Fig. 4: The CAEN educational kit full package.

The kit, shown in Fig. 4, include two γ spectrometry heads housing:

- a 3x3mm² Hamamatsu MPPC S10362-33-100C with 100 cells and breakdown voltage of 68.5V, optically coupled with 3x3x15mm³ LYSO/BGO/CsI crystals;
- a 6x6mm² SensL MicroSM-60035-X13 (18980 cells, breakdown voltage 27.35V), optically coupled with 3x3x30mm³ CsI scintillating crystal.

The analog signal generated in the SiPM is amplified by the CAEN SP5600 PSAU Power Supply and Amplification Unit [11] and sampled at 250 MS/s over a 12 bit dynamic range by the CAEN DT5720A Desktop Digitizer [12]. The DT5720A embeds an FPGA for on-board data processing, e.g. baseline calculation and charge integration. The system is controlled by a LabView based Graphical Users Interface and USB interfaced to a computer.

The proposed experiments are based on the use of the head equipped with the 6x6 mm² SensL SiPM.

IV. SNIP ALGORITHM VALIDATION

The validation of the convergence criteria for the SNIP algorithm is based on the assumption that the information in the photo-peak shall be preserved as the underlying background changes. This was established by processing ²²Na spectra

for different biasing voltages of the SiPM used to detect the scintillation light from the CsI crystal. Data were recorded for $^{22}\mathrm{Na}$ since the interaction of the two $\gamma-\mathrm{rays}$ by the positron annihilation results in a spectrum featuring a continuous and significant background to the left and right hand side of the 511 keV photo-peak.

Twelve spectra were acquired in the bias voltage range 29.8 – 31.1V. A subset is shown in Fig. 5 displaying both raw and background subtracted data. As the over-voltage is raised, the gain of the system is expected to increase together with the photon detection efficiency (PDE), the optical cross-talk and the dark count rate (DCR) [13]–[18]. As a consequence, spectra are expected to change, featuring a shift in the peak position due to the gain change and a width increase associated to the PDE variation and to a different smearing function because of the DCR and the cross-talk.

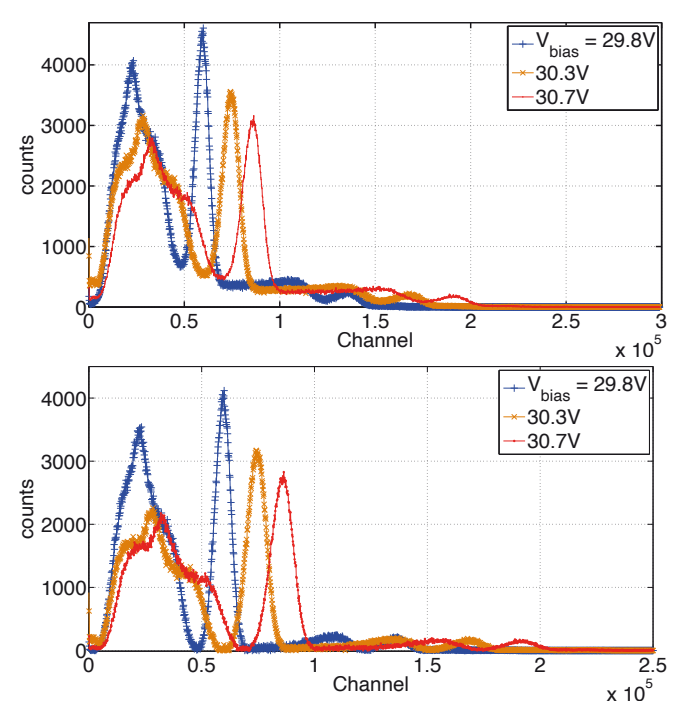


Fig. 5: Measured ²²Na gamma spectra for different bias voltages (upper panel). The SNIP processed spectra for the same subset of data are shown in the bottom panel.

After the background subtraction by SNIP algorithm, the 511 keV peak was fitted with a gaussian function. The values of the area for the different biasing conditions are presented in Fig. 6, following a normalization to the total number of events for energies higher than the back-scattering peak.

The reported errors account for the poissonian fluctuations ($\sim 0.2\%$) and the effect of the background subtraction ($\sim 1\%$). They correspond to the standard deviation of the values for a set of ten spectra recorded in identical conditions.

Effects due to the convergence criteria of the SNIP algorithm were estimated stopping the procedure one step beyond and behind the iteration corresponding to the convergence step.

The distribution of experimental areas is statistically compliant with the hypothesis of a constant value confirming that

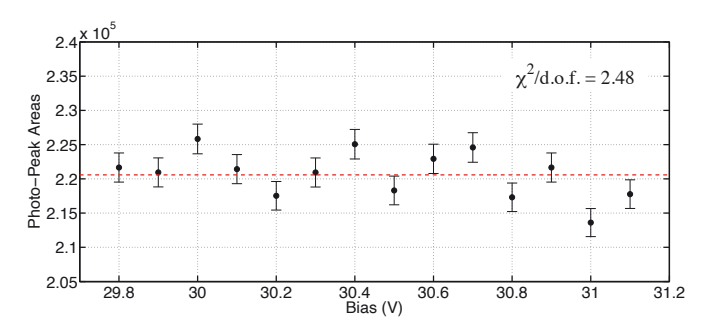


Fig. 6: Values of the photo-peak areas for different biasing conditions.

the SNIP background subtraction routine is not introducing any systematic errors.

V. MEASUREMENTS

The SNIP processed spectra from a series of sources used in educational labs (Tab. I, [19]) were used to calibrate the system response and check its linearity. Results up to the 835 keV from ⁵⁴Mn are shown in Fig. 7. The linearity of the system can be assessed, and results are shown in Fig. 7, with no indication of saturation.

TABLE I: Relevant characteristics of the used gamma isotopes.

Isotope Name	Symbol	Peak Energy (MeV)
Cadmium-109	Cd-109	0.022, 0.025, 0.088
Cobalt-57	Co-57	0.122, 0.136
Sodium-22	Na-22	0.511 (1.275)
Cesium-137	Cs-137	0.662
Manganese-54	Mn-54	0.835

Spectra were also used to verify the energy dependence of the system resolution, where a $dE/E \propto 1/\sqrt{E}$ trend can be assumed by the poissonian fluctuations in the number of scintillation photons. Data are reported in Fig. 8.

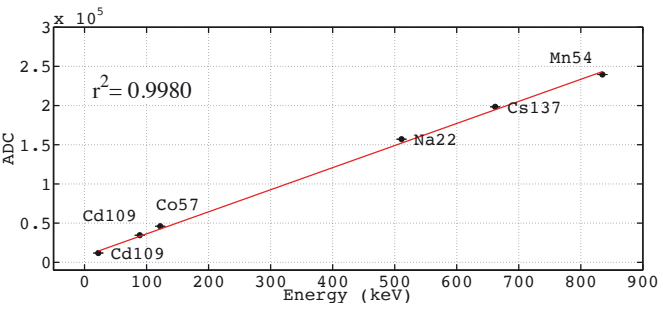


Fig. 7: Energy calibration.

The power law fit $f(E) \propto E^{-b}$ gives a value of b=0.57 \pm 0.03, in agreement with the expectations. It is worth mentioning that the resolution at the ¹³⁷Cs peak is less than 9%, at the level of the standard educational devices.

VI. CONCLUSIONS

The flexibility and the potential of the SiPM kit have been confirmed considering its configuration for gamma spectrometry. Basic measurements proving its linearity and assessing

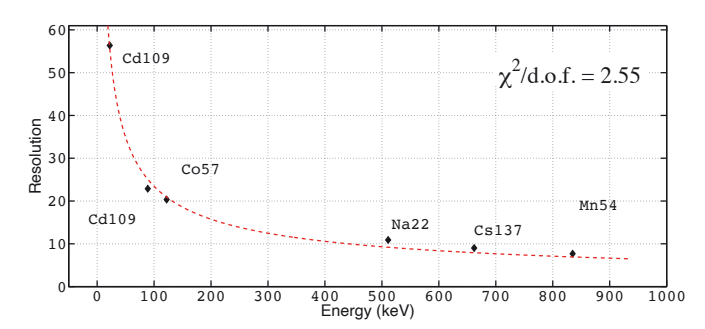


Fig. 8: Power law fit of data after the SNIP background subtraction.

its energy resolution have been performed. A MATLAB implementation of the SNIP background subtraction algorithm has been validated, providing altogether a valuable platform for entry-level experiments in gamma spectrometry tailored for undergraduate students in Physics.

REFERENCES

- M. S. Shackley, Gamma Rays, X-Rays and Stone Tools: Some Recent Advances in Archaeological Geochemistry, Journal of Archaeological Science, Volume 25, Issue 3, 1998;
- [2] M. Moussa, Gamma-ray spectrometry: a new tool for exploring archaeological sites; a case study from East Sinai, Egypt, Journal of Applied Geophysics, Volume 48, Issue 3, 2001;
- [3] Aage, H., Orsbech, U., Search for lost or orphan sources based on NaI gamma spectrometry, Appl. Radiat. Isot. 58, 103113 (2003);
- [4] Ely, J., Kouzes, R., Schweppe, J., Siciliano, E., Strachan, D., Weier, D., The use of energy windowing to discriminate SNM from NORM in radiation portal monitors, Nucl. Instrum. Methods A 560, 373387 (2006);
- [5] Ryan, C. G. and Clayton, E. and Griffin, W. L. and Sie, S. H. and Cousens, D. R., SNIP, a statistics-sensitive background treatment for the quantitative analysis of PIXE spectra in geoscience applications;
- [6] Éne, A., Badica, T., Olariu, A., Popescu, I. V., & Besliu, C. 2001, Nuclear Instruments and Methods in Physics Research B, 179, 126;
- [7] Morháč, M. and Kliman, J. and Matoušek, V. and Veselský, M. and Turzo, I., Background elimination methods for multidimensional coincidence γray spectra;
- [8] G. F. Knoll, Radiation Detection and Measurement, John Wiley & Sons (2000);
- [9] Adrian C. Melissinos and Jim Napolitano, Experiments in Modern Physics, Second Edition, Academic Press 2003;
- [10] http://www.caen.it/jsp/Template2/CaenProd.jsp?parent=61&idmod=719;
- [11] http://www.caentechnologies.com/csite/CaenProd.jsp?showLicence=false&parent=10&idmod=719;
- [12] http://www.caen.it/csite/CaenProd.jsp?parent=14&idmod=624;
- [13] D. Renker, Geiger-mode avalanche photodiodes, history, properties and problems, 2006, Nuclear Instruments and Methods in Physics Research A, 567, 48.
- [14] P. Eckert, H.-C. Schultz-Coulon, W. Shen, R. Stamen & A. Tadday, Characterisation studies of silicon photomultipliers, 2010, Nuclear Instruments and Methods in Physics Research A, 620, 217.
- [15] Y. Musienko, S. Reucroft & J. Swain, The gain, photon detection efficiency and excess noise factor of multi-pixel Geiger-mode avalanche photodiodes, 2006, Nuclear Instruments and Methods in Physics Research A, 567, 57.
- [16] Y. Du & F. Retière, After-pulsing and cross-talk in multi-pixel photon counters, 2008, Nuclear Instruments and Methods in Physics Research A, 596, 396.
- [17] M. Ramilli, A. Allevi, V. Chmill & al., Photon-number statistics with silicon photomultipliers, 2010, Journal of the Optical Society of America B Optical Physics, 27, 852;
- [18] Caccia, M. and Chmill, V. and Ebolese, A. and Martemiyanov, A. and Risigo, F. and Santoro, R. and Locatelli, M. and Pieracci, M. and Tintori, C., An Educational Kit Based on a Modular Silicon Photomultiplier System, 2013arXiv1308.3622C;
- [19] http://www.pasco.com/prodCatalog/SN/SN-7949_gamma-sources-set-of-8/#overviewTab.

